ATTITUDE CONTROL PERFORMANCE ANALYSIS USING DISCRETIZED THRUSTER WITH RESIDUAL TRACKING

John Alcorn, Hanspeter Schaub, and Scott Piggott

American Astronautical Society

39th Annual Guidance and Control Conference

Breckenridge, Colorado February 5–10, 2016

(Preprint) AAS 16-038

ATTITUDE CONTROL PERFORMANCE ANALYSIS USING DISCRETIZED THRUSTER WITH RESIDUAL TRACKING

John Alcorn,* Hanspeter Schaub,† and Scott Piggott‡

Some spacecraft rely on a cluster of thruster pairs for attitude control, momentum management, station keeping, and trajectory maneuvers. Most thrusters must be operated in a on-off control fashion. The minimum impulse bit, the smallest impulse the thruster can supply, is dictated by the minimum pulse duration of the thruster. Furthermore, the pulse duration command is discretized according to the servo frequency of the flight computer, effectively limiting the resolution of the commanded pulse duration. Each of these discrete aspects of the thruster dynamics presents a challenge when implementing a continuous control law for attitude stabilization or reaction wheel momentum management. Pulse duration residuals, that is, unimplemented thruster ON time, may be tracked and leveraged to better approximate a continuous implementation of the control law. A numerical analysis is presented of the trade space between minimum pulse duration and pulse duration resolution by characterizing performance in terms of steady state error and propellant usage in a Monte Carlo fashion. Furthermore, thruster-based torque uncertainties are taken into account to illustrate regimes where implementing the pulse residual tracking no longer impacts the final pointing performance.

INTRODUCTION

The research presented is motivated by the need for precision attitude control of spacecraft. Historically, fine pointing of a spacecraft has been achieved using reaction wheels or control moment gyroscopes and thrusters have been used as a means of coarse pointing and momentum management. However with recent advancements in thrusters and micro-thrusters, spacecraft designers are likely to put more emphasis on usage of thrusters for fine pointing. Unlike reaction wheels though, thrusters may not in general be used to implement a continuous control law due to the fact that they are not able to produce incremental levels of force. This restricts the problem to implementation of a discrete control law at a high level. A bang-bang control law is typical of a discrete system such as this, but introduces challenges regarding propellant usage and nonlinear behavior.

A continuous control law may be implemented on a configuration of thrusters in a discrete fashion without simply using a bang-bang control law.[1] Although the nominal magnitude of thrust pulse (pulse height) is constant in general, the temporal characteristics of the thrust pulse may be modulated. It is well established that when using thrusters for spacecraft attitude control pseudolinear behavior may be achieved by using Pulse-Width Pulse Frequency Modulation (PWPF) or Pulse

*Graduate Research Assistant, Department of Aerospace Engineering Sciences, University of Colorado, Colorado Center for Astrodynamics Research, Boulder, CO 80309-0431

†Alfred T. and Betty E. Look Professor of Engineering, Department of Aerospace Engineering Sciences, University of Colorado, 431 UCB, Colorado Center for Astrodynamics Research, Boulder, CO 80309-0431. AAS Fellow

‡ADCS Integrated Simulation Software Lead, Laboratory for Atmospheric and Space Physics, University of Colorado Boulder, 80303

Duration Modulation (PDM)[2] rather than bang-bang control. McClelland shows extensively that PWPF modulation consistently performs better than bang-bang control or time-optimal bang-bang control based on propellant usage, implements smoother control action, and more closely approximates a linear controller.[3] Furthermore, it is demonstrated that by avoiding the nonlinear behavior of a bang-bang controlled system that excitation of resonant frequencies of the spacecraft is commonly avoided.[4–6] A patent describes attitude control using PWPF modulation thruster control scheme and methods of hardware implementation.[7]

A fundamental set of problems not covered by previous openly published literature is the limitations imposed by flight electronics on thruster based attitude control. In general a thruster based control system is further discretized due to the temporal resolution of the pulse time command and minimum impulse bit/minimum pulse on-time. That is, any pulse duration command given to a thruster must be greater than or equal to the minimum pulse time (dictated by how fast the thruster can open/close its main valve) and must also be a multiple of the pulse time resolution (dictated by the characteristics of the flight computer and electronics associated with the thruster). These limitations mean that a linear controller will give pulse duration commands that cannot be applied due to not being a integer multiple of the pulse duration resolution. Therefore, a pulse duration command must be rounded either up, down, or to the nearest multiple of the pulse duration resolution in order to be applied. A simple mathematical algorithm for tracking residual (partial/unimplemented) thrust pulses is investigated to study how it may reduce the steady state error without impacting the desired closed loop response characteristics.

This paper presents Monte Carlo simulation results of a general one-dimensional spacecraft attitude control problem involving multiple thrusters that operate in a discrete on/off fashion using PDM and different pulse rounding algorithms including the residual tracking method. Consideration is given to performance of each algorithm and residual tracking versus a control law that includes an integral gain. Performance of each algorithm under uncertain thruster behavior is analyzed, and the sensitivity of each thruster characterizing parameter is explored. The body of the paper gives detail on the mathematical model, control algorithms, numerical simulation, and draws conclusions on the results.

PROBLEM STATEMENT

The research presented involves a general one-dimensional spacecraft with thrusters. Figure 1 gives a visualization of the problem. This section provides the equations of motion, thruster model, controller, and discrete implementation of attitude control using PDM thrusters.

Equations of Motion

Without loss in generality, this study focuses on the fixed axis rotation case to investigate how discrete thruster implementation issues impact the steady state fine pointing ability. The kinematic differential equation assumes the simple form:

$$\alpha = \frac{\mathrm{d}\omega}{\mathrm{d}t} = \frac{\mathrm{d}^2\theta}{\mathrm{d}t^2} \tag{1}$$

where α is the angular acceleration, ω is the angular velocity, and θ is the angle between the spacecraft frame and the inertial frame $\mathcal{N}$.[8,9] Each of these parameters are taken about the normal axis

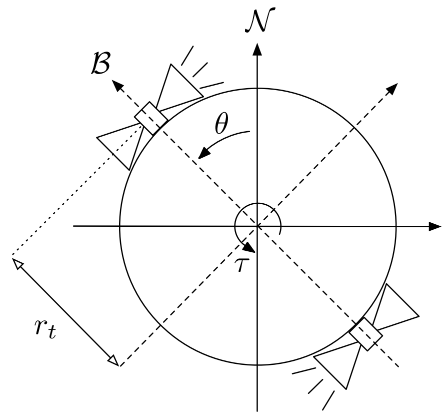

Figure 1: A simplified spacecraft with thrusters.

of the spacecraft. The dynamics of the system are governed simply by

$$\alpha = \frac{\tau}{I} \tag{2}$$

where τ is the sum of the torques applied by the thrusters and I is the inertia of the spacecraft about the normal axis.

Thruster Model

Thruster modeling errors must consider pulse-to-pulse repeatability. This is a small deviation from the nominal force a thruster produces. Pulse-to-pulse repeatability typically decreases (gets better) as the thruster "warms up" to thermal steady-state and the valves operate more consistently between consecutive pulses. For the scope of this study, the temporal variation of pulse-to-pulse repeatability are not considered as this is very small.

In addition to pulse-to-pulse repeatability, a thruster may have a static thrust bias causing it to fire either slightly hot or cold. The equation describing the actual thrust produced by a thruster is

$$F_{\text{actual}} = F_{\text{nom}} + F_{\text{bias}} + \delta F_{\text{p2p}} \tag{3}$$

where F_{nom} is the nominal force produced, F_{bias} is the static bias force (i.e. the thruster is stronger or weaker than expected), and δF_{p2p} is the deviation caused by pulse-to-pulse repeatability, where

$$\delta F_{\text{p2p}} \sim \mathcal{N}\left(0, \sigma_{\text{p2p}}^2\right) \tag{4}$$

It is assumed that the specified pulse-to-pulse repeatability β_{p2p} represents the fraction of max thrust equivalent to the 3σ value of δF_{p2p}. Thus, the standard deviation of the disturbance δF_{p2p} is given by

$$\sigma_{\text{p2p}} = \frac{1}{3}\beta_{\text{p2p}} F_{\text{nom}} \tag{5}$$

$$0 < \beta_{\text{p2p}} \tag{6}$$

Without loss in generality it is assumed that each thruster is perpendicular to its moment arm with the spacecraft center of mass. Thus, torque applied to the spacecraft by each thruster is given by

$$\tau_{\mathrm{actual}} = r_{\mathrm{t}} \cdot F_{\mathrm{actual}} \tag{7}$$

where r_{t} is the separation of the thruster from the center of mass of the spacecraft.

Control Implementation

For the research presented, the simplified spacecraft under consideration is controlled using a linear PID control law.[10] The controlled parameter is the angle θ. The control torque is given by

$$u_{\mathrm{des}} = -K\theta_{\mathrm{err}} - P\omega - K_{\mathrm{i}} \int \theta_{\mathrm{err}} \cdot \mathrm{d}t \tag{8}$$

where K is the proportional gain, P is the derivative gain, and K_{i} is the integral gain. The angle error θ_{err} is given by

$$\theta_{\mathrm{err}} = \theta - \theta_{\mathrm{ref}} \tag{9}$$

where θ_{ref} is the reference angle. Since the thrusters under consideration use Pulse Duration Modulation, the desired torque u_{des} must be translated to a pulse duration.[11] The level of thruster activity relative to maximum ℓ is related to u_{des} by the equation

$$\ell = \left|\frac{u_{\mathrm{des}}}{u_{\mathrm{max}}}\right| = \left|\frac{u_{\mathrm{des}}}{r_{\mathrm{t}} \cdot F_{\mathrm{nom}}}\right| = \frac{T_{\mathrm{p}}}{\Delta t} \tag{10}$$

Here T_{p} is the desired pulse duration and Δt is the control update period. Because ℓ is equivalent to duty cycle it must satisfy

$$0 \leq \ell \leq 1 \tag{11}$$

Rearranging equation (10) to express the pulse duration as a function of u_{des} yields

$$T_{\mathrm{p}} = \ell \cdot \Delta t = \left|\frac{u_{\mathrm{des}}}{r_{\mathrm{t}} \cdot F_{\mathrm{nom}}}\right| \cdot \Delta t \tag{12}$$

T_{p} represents the desired duration of the thrust pulse. Equation (10) shows that by applying a force F_{nom} for duration T_{p} at a frequency of $1/\Delta t$ the average torque on the spacecraft is equivalent to a case where pulse height modulation was applied. Equivalently, the total angular momentum imparted on the system is the same in each case. Thus, the most significant difference in performance is the pseudolinear behavior of pulse duration modulation compared to continuous linear behavior of pulse height modulation.

Discrete Implementations

The previous section showed that a desired torque may be translated to a pulse duration T_{p} in order to operate thrusters using PDM. Any pulse time command given to a thruster must be greater than or equal to the minimum pulse time, T_{min}, which is dictated by how fast the thruster can open/close its valve. Any pulse time must also be a multiple of the pulse time resolution, T_{res} which is dictated by the characteristics of the flight computer and electronics associated with the thruster.

Thus, T_p is discretized in order to be applied to a thruster. Define γ_f as the fractional ratio of the desired pulse duration and pulse duration resolution T_res.

$$\gamma_\mathrm{f} = \frac{T_\mathrm{p}}{T_\mathrm{res}} \tag{13}$$

This ratio is generally not a whole number. Thus, in order to implement an integer number of pulses γ_f must be rounded in some way. Four methods of rounding are investigated: FLOOR, ROUND, CEIL, and the pulse residual tracking method REM. Algorithm 1 shows the FLOOR method of rounding γ_f to obtain an applied pulse duration T_on. Using this algorithm, non-integer desired pulse ratios are always rounded down. If the desired pulse duration is less than the minimum pulse duration, T_on is rounded down to 0 and the thruster does not fire for the current control period.

Data: γ_f, T_min, T_res
Result: T_on
$\gamma_\mathrm{d} = \mathrm{floor}(\gamma_\mathrm{f})$
if $\gamma_\mathrm{d} \cdot T_\mathrm{res} < T_\mathrm{min}$ **then**
| $T_\mathrm{on} = 0$
else
| $T_\mathrm{on} = \gamma_\mathrm{d} \cdot T_\mathrm{res}$
end

Algorithm 1: Discrete thrust pulsing using FLOOR.

Algorithm 2 shows the ROUND method of rounding γ_f to obtain T_on. Using this algorithm, non-integer desired pulse ratios are always rounded to the nearest integer. If the desired pulse duration is greater than half the minimum pulse duration, T_on is rounded up to T_min. If the desired pulse duration is less than half the minimum pulse duration, T_on is rounded down to 0.

Data: γ_f, T_min, T_res
Result: T_on
$\gamma_\mathrm{d} = \mathrm{round}(\gamma_\mathrm{f})$
if $\gamma_\mathrm{d} \cdot T_\mathrm{res} < T_\mathrm{min}$ **then**
| $T_\mathrm{on} = \mathrm{round}(\frac{\gamma_\mathrm{d} \cdot T_\mathrm{res}}{T_\mathrm{min}}) \cdot T_\mathrm{min}$
else
| $T_\mathrm{on} = \gamma_\mathrm{d} \cdot T_\mathrm{res}$
end

Algorithm 2: Discrete thrust pulsing using ROUND.

Algorithm 3 shows the CEIL method of rounding γ_f to obtain T_on. Using this algorithm, non-integer desired pulse ratios are always rounded up. Desired pulse duration values less than T_min are always rounded up to T_min.

Algorithm 4 shows the REM method of processing γ_f to obtain T_on. This algorithm also tracks unimplemented thrust by retaining partial thrust pulses γ_rem. Using this algorithm, non-integer desired pulse ratios are always rounded down. The fractional pulse is retained for the next call to the algorithm. Desired pulse duration values less than T_min are always rounded up to 0, and the fractional pulse is retained.

Data: $\gamma_{\mathrm{f}}, T_{\min}, T_{\mathrm{res}}$
Result: T_{on}
$\gamma_{\mathrm{d}} = \mathrm{ceil}(\gamma_{\mathrm{f}})$
if $\gamma_{\mathrm{d}} \cdot T_{\mathrm{res}} < T_{\min}$ **then**
  $T_{\mathrm{on}} = T_{\min}$
else
  $T_{\mathrm{on}} = \gamma_{\mathrm{d}} \cdot T_{\mathrm{res}}$
end

Algorithm 3: Discrete thrust pulsing using CEIL.

Data: $\gamma_{\mathrm{f}}, \gamma_{\mathrm{rem}}, T_{\min}, T_{\mathrm{res}}$
Result: T_{on}
$\gamma_{\mathrm{c}} = \gamma_{\mathrm{f}} + \gamma_{\mathrm{rem}}$
$\gamma_{\mathrm{d}} = \mathrm{floor}(\gamma_{\mathrm{c}})$
$\gamma_{\mathrm{rem}} = \gamma_{\mathrm{f}} + \gamma_{\mathrm{rem}} - \gamma_{\mathrm{d}}$
if $\gamma_{\mathrm{d}} \cdot T_{\mathrm{res}} < T_{\min}$ **then**
  $T_{\mathrm{on}} = 0$
  $\gamma_{\mathrm{rem}} = \gamma_{\mathrm{rem}} + \gamma_{\mathrm{d}}$
else
  $T_{\mathrm{on}} = \gamma_{\mathrm{d}} \cdot T_{\mathrm{res}}$
end

Algorithm 4: Discrete thrust pulsing using residual tracking.

NUMERICAL ANALYSIS

Using the hypothetical simple spacecraft described in the previous section, the performance of Algorithms 1-4 are analyzed through numeric simulations. Analyses considered include an integral gain sweep, disturbance sensitivity, and parameter sensitivity. All simulations are run in a Monte Carlo fashion in order to obtain results that represent a span of initial angles, etc. Table 1 shows the nominal values for parameters used in the simulation. Note that some of the parameters given in Table 1 are varied in subsequent Monte Carlo simulations.

Integral Gain Sweep

The purpose of the integral gain sweep simulation is to demonstrate performance of Algorithms 1-4 under the influence of various integral gain K_{i} values. The introduction of an integral term in the control law causes steady state errors to add up until they cause another pulse to be commanded. Steady state error and impulse (propellant usage) are used as figures of merit for each K_{i} sweep. Table 2 provides parameters specific to the data given for the K_{i} sweep Monte Carlo simulations.

Figure 2 shows the Monte Carlo simulation results for Algorithms 1-4, respectively. In Figure 2(a), it is shown that using an integral gain with the FLOOR method improves performance in steady state error, but at a higher propellant cost. Figures 2(b) and 2(d) show that the ROUND and REM algorithms are largely insensitive to the inclusion of a K_{i} gain. The CEIL integral gain sweep in Figure 2(c) shows that pointing performance may be slightly improved by using an integral gain.

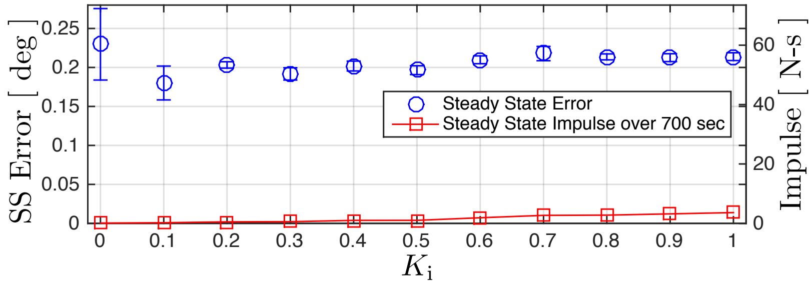

(a) K_i sweep using the FLOOR pulse rounding method.

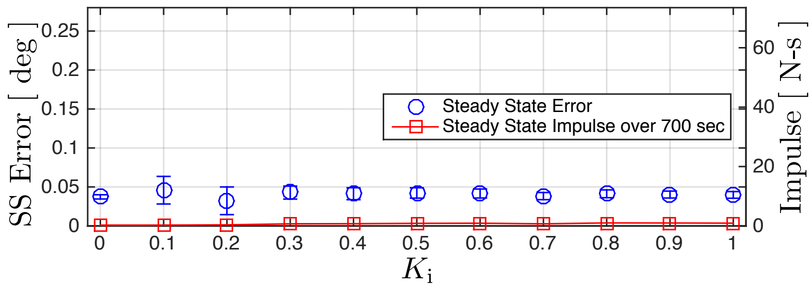

(b) K_i sweep using the ROUND pulse rounding method.

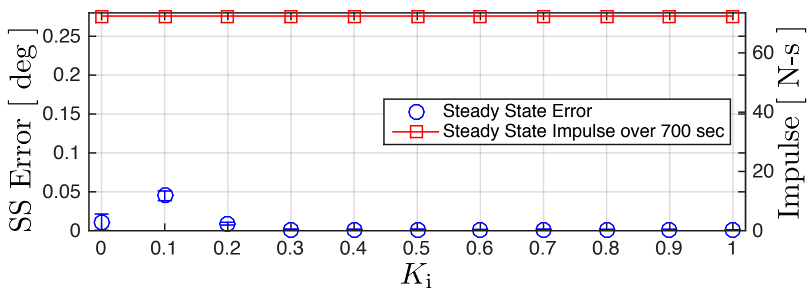

(c) K_i sweep using the CEIL pulse rounding method.

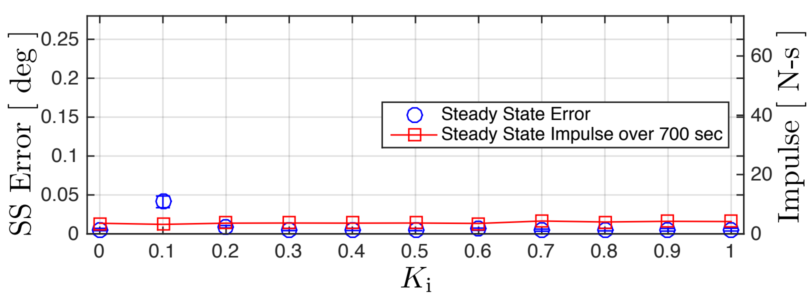

(d) K_i sweep using the REM pulse rounding method.

Figure 2: Results of the integral gain sweep analysis for each algorithm.

Table 1: Nominal simulation parameters for the simple spacecraft.

Parameter	Value	Units
Inertia, I	800	kg·m^2
Control Period, Δt	0.5	s
Proportional Gain, K	17.5580	-
Derivative Gain, P	213.3333	-
Integral Gain, K_i	0.2	-
Servo Rate	100	Hz
Nominal Thrust, F_nom	2.56	N
Moment Arm, r_t	1	m
Pulse Duration Resolution, T_res	10	ms
Minimum Pulse Duration, T_min	20	ms
Pulse-to-pulse Repeatability, β_p2p	5	%

Table 2: Monte Carlo simulation parameters for the integral gain sweep.

Parameter	Value(s)	Units
Integral Gain, K_i	$0 \rightarrow 1$	-
MC Runs Each Method	220	-

Disturbance Sensitivity

The purpose of the disturbance sensitivity analysis is to show the performance of each algorithm and each algorithm with K_i influence as an unaccounted thrust bias is applied to a thruster. Table 3 provides parameters specific to the data given for the bias sweep Monte Carlo simulations.

Table 3: Monte Carlo simulation parameters for the static bias sweep.

Parameter	Value(s)	Units
Static Bias, F_bias	-90 $\rightarrow$ 280	% of max thrust
MC Runs Each Method	260	-

Figures 3-4 show the results of the static bias sweep simulations. Figure 3 provides a comparison of the results for all methods. Note that the FLOOR and ROUND algorithms are largely insensitive to a bias. The CEIL and REM algorithms show degradation in pointing performance as a bias is added. However, when using a integral gain with CEIL, the impact on performance is not as severe. Note that the REM algorithm using integral is omitted from Figure 4(d) since it shows poorer performance in certain regimes. Figure 4 shows the same data as Figure 3 in greater detail.

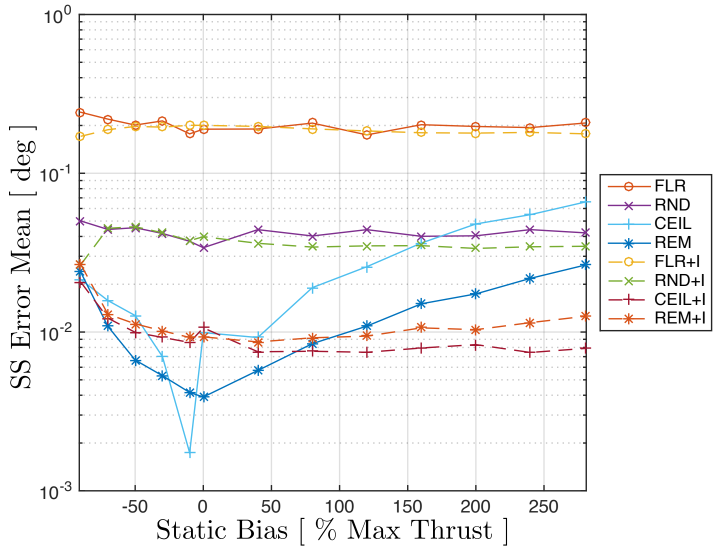

Figure 3: Static bias sweep showing results for all methods. Dashed lines indicate use of an integral term.

Parameter Sensitivity

The purpose of the parameter sensitivity analysis is to show the performance of each algorithm as minimum pulse duration T_{min} and pulse duration resolution T_{res} are varied. Table 4 provides parameters specific to the data given for the bias sweep Monte Carlo simulations. Figure 5 shows heat maps of steady state error for each of the four algorithms. From the data, it is easy to infer that steady state error is highly correlated with T_{min}. The main difference between the algorithms is sensitivity to T_{res}. Figure 5(a) suggests that the FLOOR method shows a small correlation between T_{res} and steady state error. Figure 5(b) shows that for the ROUND method the correlation between T_{res} and steady state error is very large at small values of T_{min}, and very small at larger values of T_{min}. Figure 5(c) shows that the CEIL algorithm is largely insensitive to T_{res} with the exception of a prominent "hot spot". Figure 5(d) shows that the REM algorithm is insensitive to T_{res}.

Table 4: Monte Carlo simulation parameters for the parameter sensitivity sweep.

Parameter	Value(s)	Units
Minimum Pulse Duration, T_{min}	$0 \rightarrow 500$	ms
Pulse Duration Resolution, T_{res}	$0 \rightarrow 500$	ms
MC Runs Each Method	160	-

CONCLUSION

The results show the performance of different methods of pulse rounding for discretely operating PDM thrusters. Monte Carlo simulations show the sensitivity of each algorithm to an integral

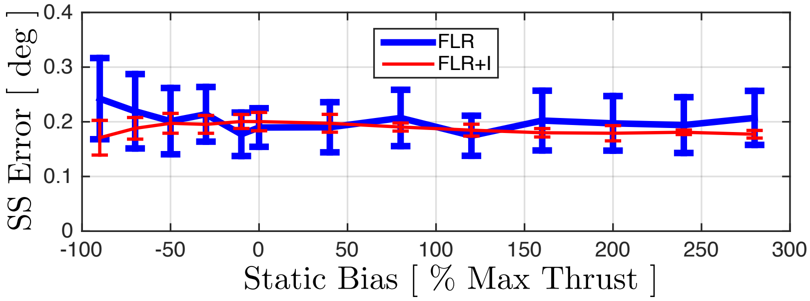

(a) Static bias sweep for the FLOOR pulse rounding method.

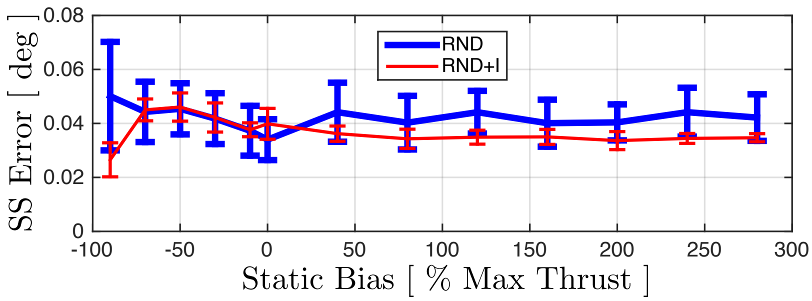

(b) Static bias sweep for the ROUND pulse rounding method.

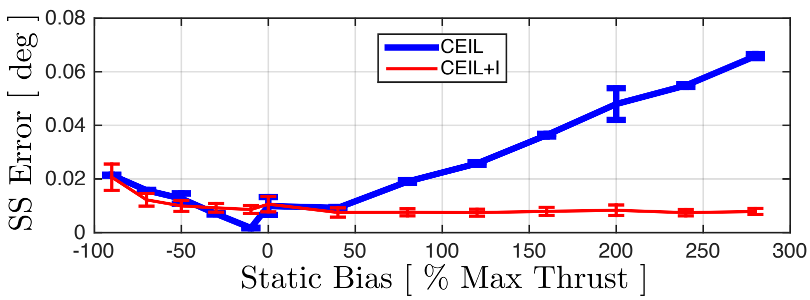

(c) Static bias sweep for the CEIL pulse rounding method.

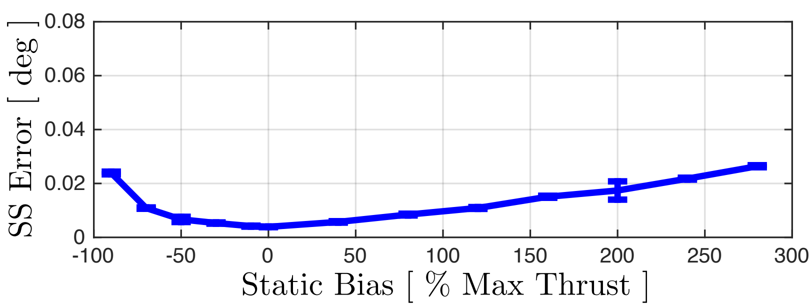

(d) Static bias sweep for the REM pulse rounding method.

Figure 4: Results of the static bias sweep analysis for each algorithm.

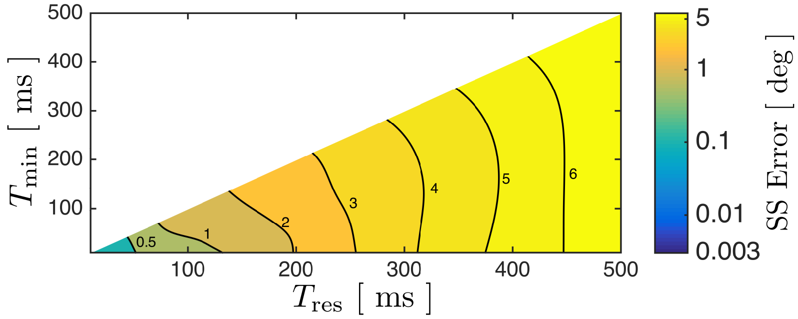

(a) Static bias sweep for the FLOOR pulse rounding method.

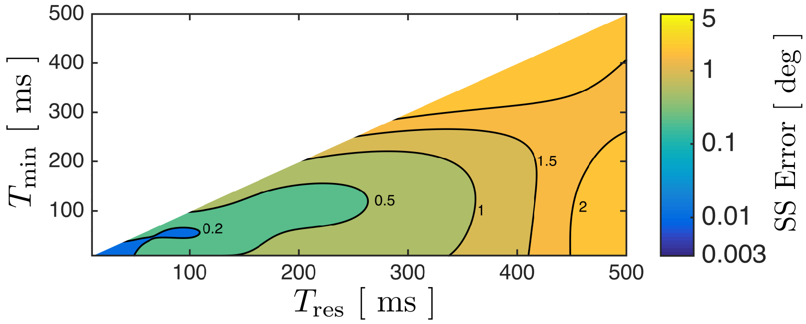

(b) Static bias sweep for the ROUND pulse rounding method.

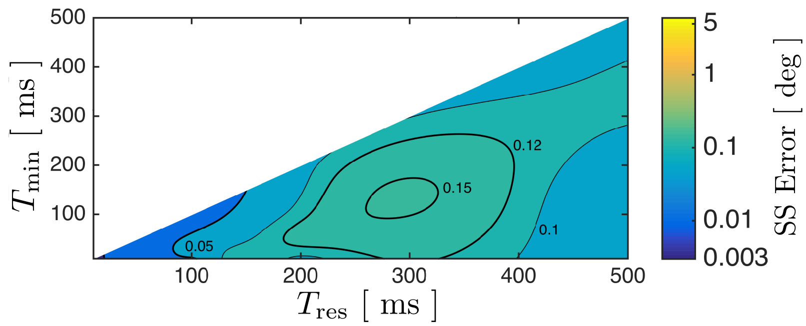

(c) Static bias sweep for the CEIL pulse rounding method.

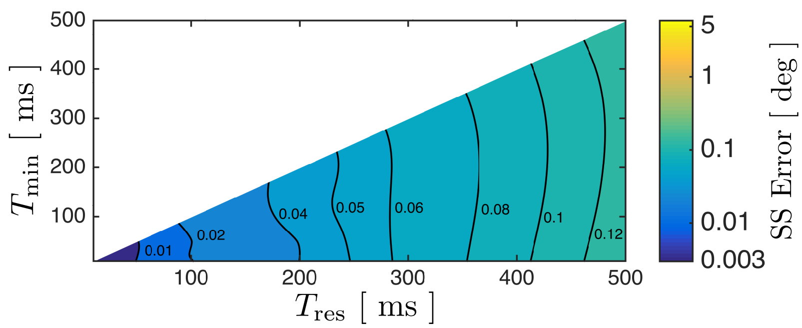

(d) Static bias sweep for the REM pulse rounding method.

Figure 5: Results of the parameter sensitivity analysis for each algorithm.

gain, static bias, and variation of timing parameters. The results show that the pulse remainder tracking algorithm REM may be used to increase steady state pointing accuracy while maintaining much lower propellant usage than other algorithms. Furthermore, the REM algorithm maintains its superior performance under large static thrust biases if an integral gain is introduced.

REFERENCES

[1] S. J. Dodds and S. E. Williamson, "A signed switching time band-bang attitude control law for fine poitning of flexible spacecraft," *International Journal of Control*, 1984.

[2] M. Barr, "Pulse Duration Modulation," *Embedded Systems Programming*, 2001.

[3] R. S. McClelland, "Spacecraft Attitude Control System Performance Using Pulse-Width Pulse-Frequency Modulated Thrusters," 1994.

[4] B. N. Agrawal, R. S. McClelland, and G. Song, "Attitude Control Of Flexible Spacecraft Using Pulse Width Pulse Frequency Modulated Thrusters," 1998.

[5] B. N. Agrawal and H. Bang, "Slew Maneuver of a flexinle spacecraft using on-off thrusters," *AIAA Guidance, Navigation, and Control*, 1993.

[6] G. Song, N. V. Buck, and B. N. Agrawal, "Spacecraft Vibration Reduction Using Pulse-Width Pulse-Frequency Modulated Input Shaper," 1999.

[7] F. N. Chan and F. C. Nilsen, "Digital PWPF Three Axis Spacecraft Attitude Control," 1986.

[8] J. R. Wertz, "Spacecraft Attitude Determination and Control," 1978.

[9] P. C. Hughes, "Spacecraft Attitude Dynamics," 2004.

[10] H. Schaub and J. L. Junkins, "Analytical Mechanics of Space Systems," *AIAA Education Series*, 2014.

[11] G. F. Franklin, J. Powell, and M. L. Workman, "Digital Control of Dynamic Systems," 1990.